

Admissible Transformation Volume for Part Dimensional Quality Gauging

Xiaoping Qian*

Mechanical, Materials & Aerospace Engineering
Illinois Institute of Technology
10 W. 32nd St
Chicago, IL 60616

Dean M. Robinson

Product Realization Lab
GE Global Research
One Research Circle
Niskayuna, NY 12309

Joseph Ross

MQTD Department
GE Aircraft Engines
One Neumann Way
Cincinnati, OH 45215

Abstract

Coordinate metrology aims to answer two questions: whether a manufactured part meets design tolerance specifications and how well the manufactured part meets the specifications. Existing methods for analyzing measured coordinate data are not adequate or effective for parts of complex tolerance zones.

This paper presents a new approach to dimensional qualification of manufactured parts. In this paper, we view the part qualification problem as an issue of finding an admissible point in transformation space. Based on the concept of admissible point, we develop theories and algorithms for part geometric dimensioning and tolerancing (GD&T) conformance check. A formulation based on containment fit for tolerance check is developed. An admissible transformation volume (ATV) is used to quantitatively characterize the quality of manufactured parts with respect to design tolerance specifications.

We examine our approach in three tolerance examples and conclude that admissible transformation volume is an effective method for part dimensional quality gauging and it is especially useful for multi-tolerance zone check where traditional methods fail to address it effectively.

1 Introduction

Dimensional inspection is a critical step in manufacturing processes to ensure manufactured parts meet tolerance specifications and perform functions as designed. Computational metrology refers to a process computationally analyzing measurement data to determine dimensional quality of manufactured parts. Two issues arise in computational metrology: whether a part meets tolerance specifications (qualitative part conformance check, a.k.a. go/no-go gauge) and how well the part meets tolerance

* Corresponding Author

The original work was done while the first author was with General Electric Research.

specifications (quantitative quality characterization). Traditionally, measurement data analysis determines if a manufactured part is conformal to tolerances specified in engineering drawings. Minimal tolerance zones are computed for simple geometry as a way of characterizing the manufacturing process quality.

A critical step in computational metrology is to align inspection data against nominal geometry, upon which the comparison can be drawn. Two popular approaches (total least-squares and minim-max best fit) for aligning inspection data against nominal model do not necessarily reflect true design intent of tolerance specifications. For example, a least-squares method may produce incorrect tolerance conformance check result when it is used to align inspection surfaces against nominal surfaces of non-uniform tolerance. Simple zone fitting only leads to a pass/fail description of the manufactured shape against design tolerance specifications.

The state-of-the-art coordinate data analysis methods are also limited in methods to characterize how well the part meets tolerance specification. Existing dimensional quality analysis methods are based on either the deviation between as-measured part data and the nominal model or the minimal tolerance zone of the measured data. These methods are either not conformal to ANSI Y14.5M standard [1] or not directly applicable to complex tolerance such as non-uniform tolerance and composite tolerance. Some of these methods are dedicated to particular classes of tolerances and are computationally undesirable. For example, only limited methods available for calculating minimal tolerance zones of simplex geometry. Furthermore, these methods cannot quantitatively evaluate part dimensional quality when multiple tolerance requirements need to be simultaneously met.

As more and more dimensional measurement systems such as trigger probe coordinate measurement machines (CMM), scanning CMMs and optical scanning systems become readily available, there is an increasing need for quantitative feedback of inspection data analysis results so that this information can be used for manufacturing processes improvement.

This paper presents a new approach for dimensional inspection data analysis. It analyzes inspected dimensional data in transformation space. It employs a novel concept, *admissible transformation volume (ATV)*, to quantitatively evaluate how well the manufactured part fits into the design tolerance zone. Advantages of this approach are as follows:

- It **conforms to design intent** of tolerance specifications since it directly examines whether a part shape falls within the tolerance zone.
- It is **applicable to all classes of geometric dimensioning and tolerancing (GD & T)** that can be represented in tolerance zones. In contrast to many previous minimal tolerance zone calculation methods, which are dedicated and only applicable to a particular type of tolerance such as cylindricity or flatness. The ATV method is applicable to tolerance zones of all types of tolerances.

- It is **useful for inspection of complex shapes of non-uniform tolerance zones** where existing methods do not apply. Since a minimum tolerance zone is based on two surface envelopes offset from one ideal geometry, it is not applicable to tolerances of multiple tolerance features, or composite tolerances. Figure 1 illustrates an example of non-uniform tolerance zone and an inspection point data set. In such a case (where multiple tolerances are used to define tolerance zone), minimal tolerance zone is not uniquely defined and cannot be directly used to characterize manufacturing process capability.

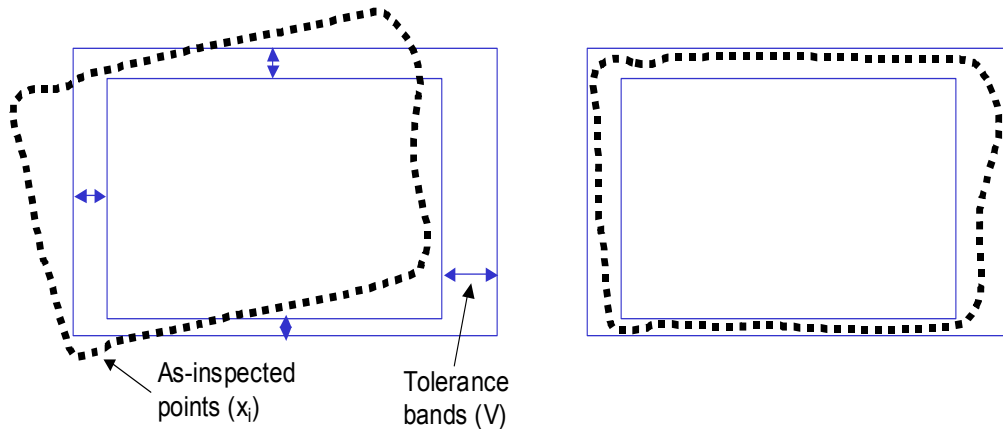


Figure 1 Non-uniform tolerance zone and inspection data analysis

In the rest of this paper, we review prior work in measurement data analysis in Section 2. We present the theory and algorithms of applying admissible transformation for part GD& T conformance check and conformance allowance computing in Section 3 and Section 4. Experimental results are listed in Section 5. This paper concludes in Section 6.

2 Literature Review

Part dimensional quality analysis requires the comparison of measured part coordinate data with respect to part GD&T specifications. GD&T is an important technology in product design and manufacturing. Through GD&T, design intent can be represented, part quality can be analyzed, part interoperability from different manufacturing processes and vendors can be ensured, and manufacturing cost can be reduced.

Functional and assembly requirements on the manufactured parts are represented as tolerance zones to which the surface of a part must conform. These geometric tolerances are defined in the ASME Y14.5M-1994 geometric dimensioning and tolerancing standard [1]. Based on the standard, tolerances are to be evaluated from envelopes of two ideal features with minimum separation distance within which the entire surface of the manufactured part must lie.

To analyze whether a manufactured part meets design tolerance specifications from a set of part coordinate data, one needs a proper representation of tolerance and an appropriate methodology to compare measured coordinate data with the tolerance. Such comparisons

are used not only to determine the qualification of the manufactured part, but also to extract quantitative part quality information that can be fed back for process modification as well as design change for producibility improvement.

In this section, we briefly review GD&T theories as well as methods to construct tolerance zones. We then present past and current methods on part dimensional quality analysis.

2.1 Geometric dimensioning and tolerancing theories

Manufactured parts have deviations from the nominal shape. To describe and preserve the functional requirements of design, geometric variations are specified in tolerance zones. Pasupathy et al gave a comprehensive review of various existing tolerance zone construction methods in [20].

Offset zone models modeled as Boolean subtraction of maximal and minimal object volumes have been explored by Requicha [23] and Roy [24]. Turner developed indirect parameterization methods for modeling tolerance zones [27]. A Technologically and Topologically Related Surfaces (TTRS) method was developed by Clement [8], where they used group theory and displacement torsors to combine the surfaces into 28 different geometric relationships. Shah and Zhang developed a graph-based model for geometric tolerancing by separating linear variations from angular variations based on degrees of freedom for points, lines, and planes [26].

Recently Davidson and Shah proposed a new mathematical model, Tolerance-Map, a hypothetical volume of points that corresponds to all possible locations and variations of a segment of a plane which can arise from tolerances in size, form, and orientation [10]. A GD&T global model for computerizing GD&T representation was reported in [29].

In this paper, we focus on developing a measure of part dimensional quality in its conformance to GD&T specifications. We assume the tolerance zone Z is represented as a parametric function of nominal geometry S . That is, for a given surface point in its parametric representation $S(u,v)$, we can compute the tolerance zone $Z(u,v)$ at that point. The methodology and the metric developed in this paper are applicable to other tolerance representations as well.

2.2 Dimensional quality analysis from measurement data

Dimensional quality analysis of measured coordinate points serves two important purposes: 1) to check whether a manufactured part meets design GD&T specifications (*qualitative GD& T conformance check*), 2) to characterize manufacturing process capability and examine how much space remains for a manufactured part shape to stay within a tolerance zone (*quantitative characterization of part dimensional quality and process capability*). The first question concerns whether a manufactured part meets design tolerance specification. The second question concerns whether the manufactured part just fits into a tolerance zone or if there is ample space remaining. This quantitative characterization of part quality is critical for improving part producibility. Part

dimensional quality is often evaluated based on the minimum tolerance zone computed from the measured dimensional data. This evaluation is often based on numerical fitting algorithms that transform the measured coordinate data into the nominal geometry's coordinate system to minimize the deviation between the nominal shape and the inspection point set. The fitting algorithms can be largely divided into two types: least-squares fit and mini-max fit. Refer to Feng [12] for a detailed review of various fitting algorithms.

An alternative to the numerical fitting algorithms is a combinatorial search for particular points that control and govern the minimum tolerance zone. In addition, manual fitting is still employed for some complex and high precision part inspection.

We now review these dimensional quality analysis methods and explain why our proposed approach is advantageous for part dimensional quality analysis.

2.2.1 Numerical fitting based tolerance evaluation

The numerical fitting based methods are relatively easy to implement and are applicable to a variety of GD&T classes. In general, these methods are fast but subject to potential errors due to numerical approximations and the lack of true global optimization algorithms.

Least-squares fit

The total least-squares fit aims to find optimal parameters to minimize the total deviation between an inspection point set and a nominal model. Total least-square fitting calculates deviation for all the inspection points and then sums its deviations. For example, Menq used this method for surface profile inspection [18].

Mathematically, it is represented as

$$\text{Min } \left(\sum_{i=1}^N (T(x_i, t) - s(u, v))^2 \right) \quad \text{EQ. 1}$$

In this equation, $T(x_i, t)$ represents the inspection points after the transformation, t is the transformation parameter, $s(u, v)$ representing nominal geometry, x_i ($i=1, \dots, N$) is an inspection point with N the number of points in the inspection point set.

Total least-squares fitting is the most widely used approach in CMM data analysis. However, it does not always produce results conformal to design intent, especially for non-uniform tolerance. Total least-squares fitting minimizes the overall root-mean-square error, but may lead to a larger maximum deviation. Therefore total least-squares fitting could over-estimate the tolerance values, which would unnecessarily disqualify many otherwise qualified parts.

Mini-max fit

To resolve the inconsistency between design intent of tolerance specifications and the least-squares fit, an alternative fitting method, minim-max fit, has been developed. It aims to find an optimal alignment to minimize the maximum deviation between the nominal model and an inspection point set. Minimum tolerance is then computed based on the maximum deviation between the nominal geometry and the measured point set. For example, Murthy used a Monte Carlo simulation algorithm to determine the minimal tolerance zone for form tolerance [19]. Lai modified a genetic algorithm for calculating the minimum-zone for cylindricity [16]. Endrias proposed the usage of rigid-body coordinate transformation to seek the minimum-zone for form tolerance, in which only necessary independent transformation parameters were used in the minimal zone optimization process [11].

Mathematically, it is represented as

$$\text{Min}(\max(\text{fabs}(T(x_i, t) - s(u, v))) \quad \text{EQ. 2}$$

Mini-max fit is useful for estimating tolerances such as roundness, cylindricity and flatness. It is not directly applicable to shapes with non-uniform tolerance bands, or with asymmetric tolerance bands. Mini-max fitting minimizes the largest deviation error but it may lead to alignment with larger overall root-mean-square error. It is also computationally undesirable since the first derivative of the objective function may not be continuous.

Zone fit

Recognizing the deficiencies of the two types of fitting algorithms, Choi and Kurfess developed a zone-fitting algorithm [6], in which a quasi-Newton method is used to numerically seek a rigid body transformation placing the inspection points inside the tolerance zone. Since a simple zone fitting only produces a binary decision regarding the GD&T conformance, they extended this method for minimal zone computing to quantitatively characterize part quality. They proposed a two-stage zone-fitting algorithm, which iteratively optimized the coordinate transformation parameters until a minimum-zone solution was obtained [7]. Even though a minimum tolerance zone is an effective metric for part quality characterization, it becomes ineffective when multiple tolerance zones are involved. When multiple tolerances have to be simultaneously met, the minimal tolerance zone of a tolerance feature may vary when the value specification of other tolerance zones changes. To address this issue, a conditional tolerance zone concept is proposed in [7]. The minimum tolerance zone for a tolerance feature is computed while holding a constant tolerance zone on the other tolerance features. This would unfortunately lead to multiple minimum tolerance zone values for a given tolerance feature. It would also involve combinatorial evaluation of minimal tolerance zones for multiple tolerance features.

The admissible transformation is similar to the zone fitting method in that both approaches compare inspection points with a tolerance zone. However, we explicitly

quantify the amount of admissible transformation (ATV) in the transformation space and examine quantitatively the ATV change due to design tolerance specifications change and manufacturing error variation. As such, ATV is applicable to both single and multiple tolerance zone specifications.

2.2.2 Combinatorial minimum zone computing

Various geometric approaches have also been explored to calculate the minimal tolerance zone. In these approaches, points that control the minimum tolerance zone are explicitly identified. Huang used a method called control line rotation scheme to identify points to calculate minimum-zone straightness [12]. Damodarasamy used a normal plane method and simplex search for calculating the minimum zone for flatness [9]. Roy and Zhang constructed the nearest and farthest Voronoi diagrams of a data set for circularity evaluation [25]. The minimum tolerance zone issue has also been formed as an annulus placement issue in computational geometry [2].

Due to the combinatorial nature of these algorithms, they are computationally expensive and are dedicated to particular types of tolerances and not applicable for general classes of tolerances.

Manual fit

Besides the above automatic fitting methods, another method that is often used in checking part dimensional quality is through the use of manual fit. In this method, a blueprint drawing with the tolerance zone is magnified and printed on a Mylar or plastic paper. The actual part profile is then superimposed against the blue print. The operators then manually move the part profile against the tolerance zone in the blue print. If the part profile can be placed inside the tolerance zone, the part is considered “pass”. Otherwise, it is considered “fail”. The advantage of this approach is that it conforms to design intent of tolerance specifications. However, despite its wide usage in high precision and complex profile part inspection, this method also has many disadvantages. It is subjective, not repeatable, and relies on operators’ judgment. When the shape is very complex or the actual shape is very close to the tolerance zone boundary, it is very difficult for operators to move the part into the tolerance zone even if the actual part is a dimensionally qualified part. More importantly, this manual fit method can only determine whether a part meets tolerance specifications, and it does not provide any information regarding how well the part meets tolerance specifications.

Similar to this manual fit, a geometric framework was developed to quantify the structure of positional tolerance evaluation [15]. A comparison between a genetic search method and a generalized reduced gradient method was done to explore methods for automatic analysis of inspection points for complex classes of objects [4].

In summary, so far there is a lack of an effective measure of part dimensional quality that is applicable to a variety of GD&T classes and conformal to ANSI Y14.5M standard. The current practice using the minimum tolerance zone as a quality measure is computationally undesirable. Furthermore, it is not directly applicable to complex

tolerances because the minimum tolerance zone characterizes part quality only through two surface envelopes offset from one ideal geometry and complex tolerances often involve more than one tolerance feature. In this paper, part dimensional quality is quantified based on the amount of allowable transformation upon which a manufactured part shape remains within the tolerance zone. Such a measure is applicable to all GD&T classes where tolerance zones can be non-uniform, complex, or composite.

3 Theory on Transformation Space for Inspection Data Analysis

In this section, we describe a) the concept of an admissible transformation point, b) how this concept is utilized in containment fit for part dimensional tolerance conformance check, and c) how it is used in ATV computing for conformance allowance check as a way of characterizing part dimensional quality with reference to the tolerance zones.

The basic premise underpinning our approach is that the issue of part GD&T conformance check can be transformed into an issue of whether there exists a transformation such that, upon this transformation, the inspection points can be contained in the tolerance zone. Geometrically speaking, this is essentially a containment problem.

We can further extend this containment concept into how well the inspection points fit into tolerance zone. Instead of calculating minimal tolerance zones, we calculate the allowed amount of movement (translation and rotation) of the inspection points such that these points can still be contained in the tolerance zone.

In this paper, we assume the inspection point set represents the actual manufacturing shape. So we use the term inspection point set and manufactured shape interchangeably in this paper. In addition, we do not consider measurement uncertainty in this paper.

3.1 Parametric tolerance zone representation for part qualification

In order to conduct a containment check, an efficient representation of tolerance zone is needed. In this paper, we represent the tolerance zone as a distance function of nominal geometry. If the part surface has parametric representation $s(u,v)$, we can then have tolerance zone represented as

$$Z = Z(u, v)$$

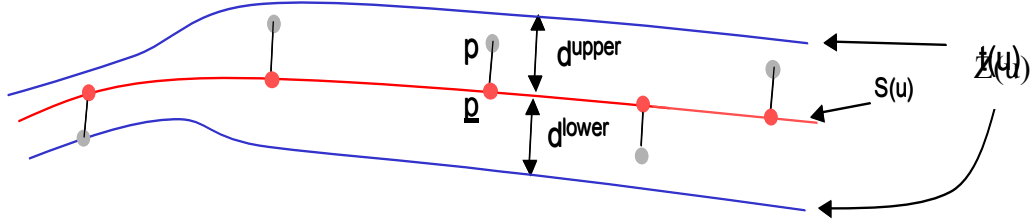


Figure 2 Parametric representation of tolerance zone

That is, given a surface point and its parameter set (u, v) , we can calculate the tolerance band from the parameter set. Figure 2 illustrates a 2D example. For any given point p_i , we can find the closest point $\underline{p}_i(u_i, v_i)$ in the nominal surface. At this closest point, the tolerance can be represented as an interval $[d_i^l, d_i^u]$, which could be a symmetric two-sided tolerance, or asymmetric tolerance, or one-sided tolerance. We note the distance between the point p_i and the nominal geometry as a signed distance d

$$d = |p_i - \underline{p}_i| \cdot \tau$$

τ equals 1 if $\overrightarrow{\underline{p}_i p_i}$ has the same direction as part surface normal at point p . Otherwise, τ equals -1 . So the point p_i lies within tolerance zone if and only if $d \in [d_i^l, d_i^u]$. The manufactured part meets tolerance specification if and only if all inspection points fall within the tolerance zone.

3.2 Degrees of freedom and admissible transformation

If we represent tolerance zone as a set Z in an N -dimensional Euclidian space R^n , $n=2, 3$. Its boundary representation is described as a distance function from the nominal shape. Its coordinate system is represented as F_D , meaning a reference frame in design coordinate system.

The inspection point set is represented as P in the coordinate system F_I (a reference frame in inspection coordinate system). We assume if all the points in the point set P can be fit into the tolerance zone Z , the part is then conformal to part tolerance specifications. This can be formed mathematically as a containment problem as following: Given two sets P and Z , a part is conformal to tolerance specification if and only if under a transformation t such that P is contained within Z ,

$$T(P, t) \subset Z$$

To better describe the process of computing such a transformation, we define a transformation space first.

For n degrees of freedom, we define an n -dimensional *transformation space* R^n , $n=1, 2, \dots$.
6. A more general representation of a point in the space could be $(x, y, z, \theta, \phi, \gamma)$,

respectively representing three translation components and three rotation components around x, y, and z axes. Each point in this transformation space represents a point T_i . These degrees of freedom correspond to the movement range if a part needs to be moved and qualified manually. A free rigid body has six degrees of freedom, three in translation and three in rotation. In the context of part GD&T conformance check, the degrees of freedom in fitting inspection data against nominal model/tolerance zone could be less than six. For example, a minimum deviation zone of a straightness tolerance can be obtained by optimizing a one-parameter objective function. In the case of manual inspection of a surface profile through the optical comparator, there are three degrees of freedom for profile tolerance conformance check. They are two translations (x and y) and one rotation around the z-axis (θ). A point in such a transformation space represents a transformation (x_i, y_i, θ_i) applied to the measured point cloud P (Figure 3).

A point is an *admissible transformation point* if and only if such a transformation leads to the measured point set P falling within tolerance zone Z.

A collection of all such admissible transformation points is called *admissible transformation volume (ATV)*. It is a measure of the allowed movement amount for inspection point set such that this set remains within the tolerance zone.

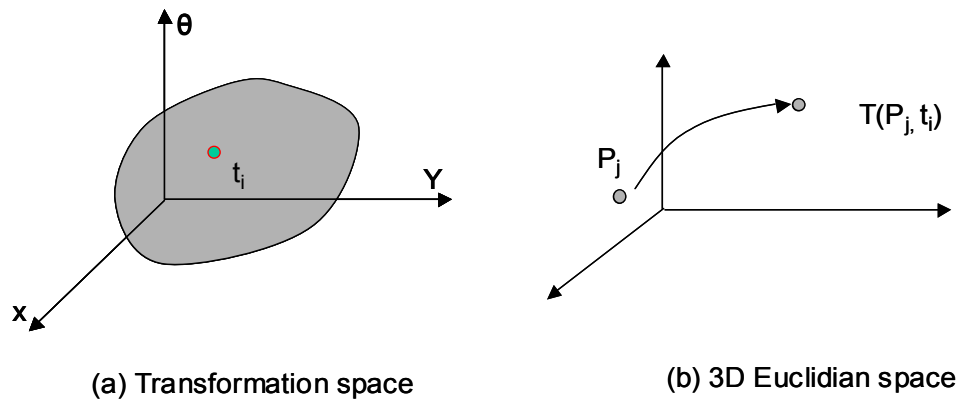


Figure 3 Transformation Space

3.3 Containment fit

In order to find an admissible point in the transformation space and to define the boundary of the admissible transformation volume, we define a distance function in the 3D nominal model's Euclidian Space. In this paper, we define the containment fit function as the average point distance between the points outside the tolerance zone and the tolerance zone boundary (Figure 4). That is, we only count the points outside the tolerance zone.

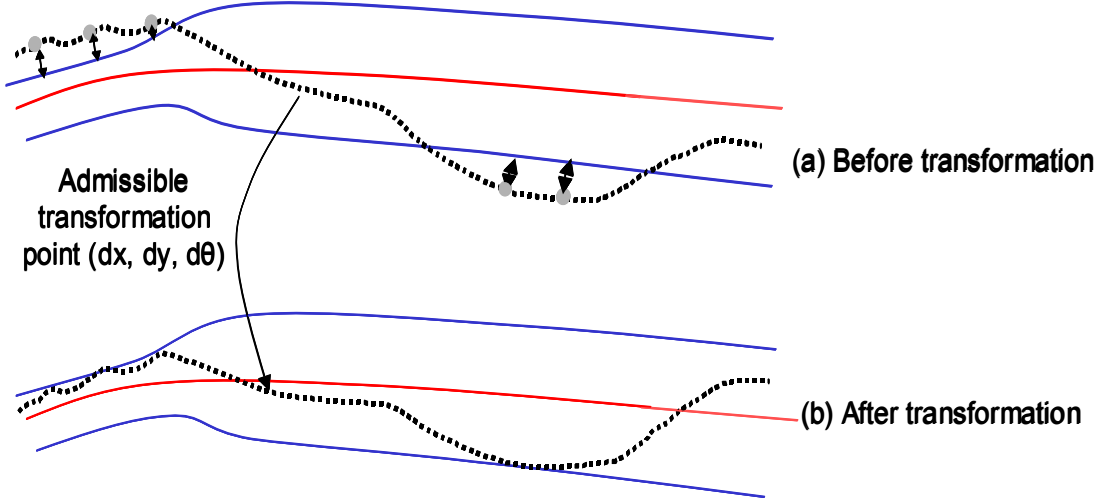


Figure 4 Containment Fit

Mathematically, the objective function is defined as follows

$$f = \sqrt[m]{\frac{\sum_{i=1}^N \|g(T(p_i, t) - s(u, v))\|^m}{N}} \quad \text{EQ. 3}$$

$$g(T(p_i, t) - s) = \begin{cases} 0 & \text{if } d \in [d_1, d_u] \\ |d - d_1| & \text{if } d < d_1 \\ |d - d_u| & \text{if } d > d_u \end{cases} \quad \text{EQ. 4}$$

In the above equations, t is transformation coordinates, $T(p_i, t)$ represents a transformation of point p_i by t . If t is a point in six-dimensional transformation space, $t = (x, y, z, \theta, \phi, \gamma)$. N is the total number of points in the inspection point set. The symbol m represents the order of distance function g in the containment fit. When $m=2$, it is the root-mean-square (RMS) distance for points outside the tolerance zone. It is also the same function used in [6]. However, our containment fit function essentially minimizes the L_m norm with m extendable from $m=1$ to $m=\infty$. In this paper, we also examine the computing of containment fit and ATV for $m=1$ and $m=3$. In this formulation, the actual part quality is not dependent on the choice of m , however, larger m leads to better convergence for some numerical algorithms. In EQ.3, when m increases, the gradient also increases, which would lead to larger objective function value differences for a given pair of points in transformation space. As it turns out in our implementation, a simplex method using smaller m in the objective function leads to the iterative process terminated prematurely due to its smaller value difference among the vertices.

For any given set of parameters (in the transformation space), if the objective function is zero, this transformation point is an admissible point. If the minimal objective function value is not zero, the part is out of tolerance specification. The minimal value is an indication of how much the part is out of tolerance specification. The objective function f is a measure of the average distance between points outside of point boundary and the tolerance boundary.

If the objective function is larger than zero, it means under this transformation t_i , inspection points are still f distance away from lying within the tolerance zone. A collection of the transformation points that would lead to the same objective function value is called (hyper) iso-surface. If there are two degrees of freedom, such a collection would be an iso-curve. If there are three degrees of freedom, it would be an iso-surface. When there are more than three degrees of freedom, such a point set forms a hyper-iso-surface.

When the objective function value is zero, the corresponding iso-surface and the enclosed area in the transformation space form the ATV. We adopt a functional representation of the boundary of admissible transformation volume. That is,

$$f = \sqrt[m]{\frac{\sum_{i=1}^N \|g(T(p_i, t) - s(u, v))\|^m}{N}} = 0$$

This function describes exactly the boundary representation of such a geometric shape in transformation space.

By computing the iso-surface and ATV, we can derive part quality information with respect to the design specified tolerance zone.

The ATV as a part dimensional quality metric relates to minimal tolerance zone in the following way. An ATV reflects the comparison between an actual part shape and design tolerance specification, while a minimum tolerance zone is a minimal zone bounding the tolerance feature regardless of design tolerance specification value. As minimal tolerance zone gets smaller, ATV gets smaller. When the minimal tolerance zone of a part is smaller than design specified tolerance, there exists an ATV for this part. When the minimal tolerance zone is the same as design specified tolerance zone, the ATV is degenerated into a point. When the minimal tolerance zone is larger than the design tolerance specification, ATV is NULL and a volume enclosed by the hyper-iso-surface in the transformation space is used as a characterization of how bad the part quality is. However, minimal tolerance zone is ineffective in handling simultaneous multiple tolerance zone specifications and multiple tolerance zone values may exist for one tolerance feature depending on the tolerance zone value for other tolerance features. ATV, as a single metric, is applicable to both single and multiple tolerance zone specifications.

3.4 Propositions for Admissible Transformation Volume

Compared to traditional methods in characterization part dimensional quality, the ATV based approach is more conformal to design intent of tolerance specifications than many other best fit based methods since it directly finds a transformation which places the inspection point set within the tolerance zone.

An ATV is a geometric representation, representing the intrinsic geometric relationships between tolerance zone and manufactured part shape. It is not dependent on containment functions or the initial positions of the manufactured shapes. It is only dependent on the design specified tolerance zone and manufactured part shape.

Based on the definition of the ATV in the transformation space, we have the following propositions for ATV.

Proposition 1: A manufactured part is within tolerance specifications if and only if its admissible transformation volume is not null. That is,

$$ATV \neq \emptyset \Leftrightarrow \text{Pass}$$

This proposition implies:

- When an admissible transformation volume is null, the manufactured part is out of tolerance specification and vice versa.
- When an admissible transformation volume is not null, the manufactured part is within tolerance specification, and vice versa.

This proposition is the underlying principle for our inspection data analysis approach. We seek to check the existence of an admissible transformation volume to determine the manufactured part dimensional quality with respect to tolerance specifications.

Proposition 2: The Minkowski sum of admissible transformation volume for a fixed orientation in transformation space and the inspection point set is a subset of the tolerance zone.

Proposition 3: The larger a tolerance is, the larger a nominal model's admissible transformation volume is. That is

$$\text{If } \delta_1 < \delta_2, \text{ then } V_{ATV1} < V_{ATV2}$$

If two parts of same nominal geometry, one has tolerance δ_1 smaller than the other tolerance δ_2 , then the first part's ATV is larger than the second ones. Here we use the volume of ATV as a measure of the ATV. For example, for transformation space (x, y, θ) of three degrees of freedom, the volume is defined mathematically as

$$V = \iiint_{ATV} dx dy d\theta$$

Within the ATV, the EQ. 3 $f(t)$ equals to zero. As the tolerance of nominal geometry becomes larger, so does the tolerance zone. It in turn allows the nominal shape to move further yet still within tolerance zone. Thus it would lead to a larger ATV for the nominal shape.

Proposition 4: A manufactured part's minimal tolerance zone has the same size as design specified tolerance zone if and only if the ATV is degenerated into a point.

When an ATV only contains a point, any deviation from this transformation point, the manufactured part would fall out side of tolerance zones. Otherwise, the manufactured part's minimal tolerance zone would be larger than the design specified tolerance zone.

When an ATV contains more than one point in its neighborhood in the transformation space, it means the manufactured part can deviate from a given position while still remain in the tolerance zone. It means this part has a minimum tolerance zone smaller than the design specified tolerance.

Proposition 5: The nominal design shape's admissible transformation volume ATV_D should be no smaller than the actual manufactured shape's admissible transformation volume ATV_M . That is

$$V_{ATVD} > V_{ATVM},$$

Since no manufacturing process is perfect and without dimensional deviation, the manufactured shape always has deviation from nominal geometry. If a manufactured part can move more than a nominal geometry can yet both stay within tolerance zone, then the tolerance is not properly defined.

Proposition 6: The ATV is independent from the choice of coordinate system frame of design shape F_D and inspection point set F_I , even though its specific position and orientation are dependent on the initial reference frame. The shape of the volume is independent from the initial reference frame.

Since ATV contains a set of transformation, by which the manufactured shape stays within tolerance zone, the tolerance zone is completely determined by the design shape, the ATV is only dependent on the manufactured shape and the nominal tolerance zone. So ATV is an intrinsic property of the manufactured shape with regarding to the tolerance zone. It does not depend on the choice of the coordinate system.

Proposition 7: The ATV is independent from the containment objective functions.

Containment fit objective functions as listed in EQ.3 only serves to mathematically describe the boundary of ATV. The ATV is independent from the specific form of the containment fit function.

The objective function for containment fit could also be a minimal maximum function for points outside tolerance zones.

$$f = \text{Min}(\max\|g(T(p_i, t) - s(u, v))\| \quad \text{EQ. 5}$$

EQ.5 and EQ.3 would produce the same shape for the ATV. However, mini-max objective functions tend to have more local minimum.

4 Algorithms for Containment Fit and ATV Computing

Based on the ATV concept, we will address how this concept is utilized in both part conformance check (go/no-go gauging) and part conformance allowance calculation for manufacturing process capability characterization. The overall flowchart of inspection data analysis based on ATV is shown in Figure 5. The input of this process includes nominal shape, inspection data and tolerance zone. Nominal shape is used to compute the ATV for the nominal geometry and to calculate the distance to the inspection points. The output of this process includes whether the manufactured part meets design tolerance specifications and how well it meets the specifications

This process involves three basic algorithms: distance calculation between inspection points and tolerance zone boundary, containment-fit objective function minimization and ATV computing. Since this part conformance is formed as a containment-fit problem, we use simplex search to check if the part falls within part tolerance specification. A least-squares method to minimize the deviation between the nominal shape and the manufactured shape can be used initially to transform inspection data closer to nominal geometry. This would lead to fewer iterative times for simplex search. The nominal shape's ATV can provide initial conditions for simplex vertices in the simplex search for manufactured parts' conformance check. To calculate a manufactured part's conformance allowance, we use the Marching Cubes algorithm to calculate both nominal shape and as-inspected shape's ATV.

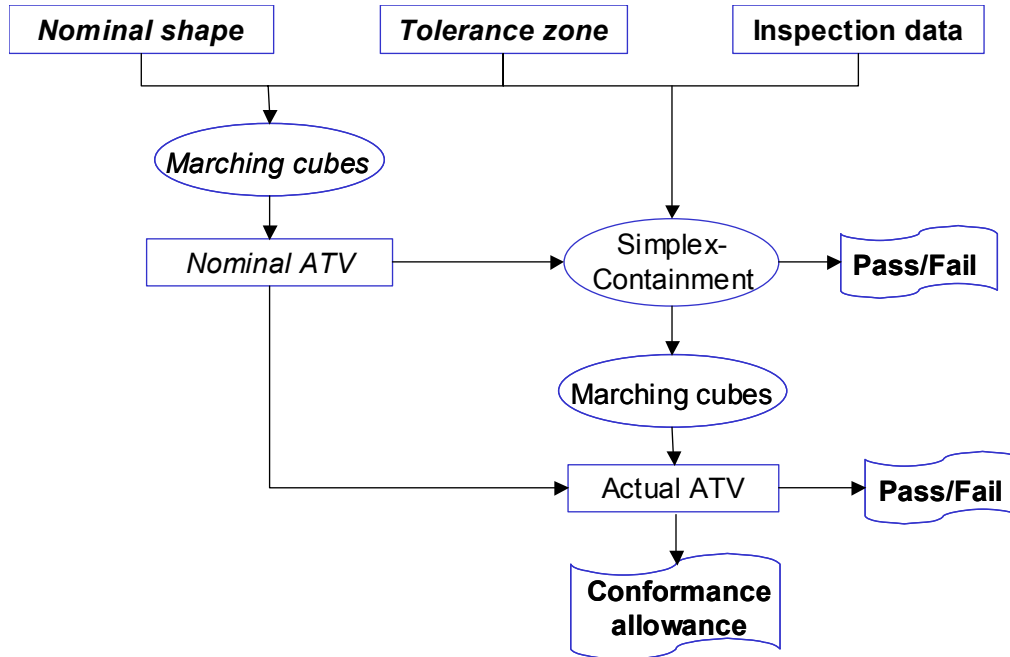


Figure 5 Flowchart for inspection data analysis

We now detail the three algorithms as follows.

4.1 Inspection point and tolerance zone distance calculation

Containment fit requires the calculation of distance between a set of inspection points and design specified tolerance zone. Naïve implementation of such a containment check would compare each inspection point against all the boundary surfaces of the tolerance zone to determine if an inspection point fits into the tolerance zone.

In this paper, we represent the tolerance zone as a function of parametrized representation of nominal geometry. That is, if the nominal geometry has the parametrization $s(u,v)$, we can represent the tolerance zone as $Z = Z(u,v)$. For each inspection point p , we calculate the closest point \underline{p} in the nominal geometry, we then calculate the distance between point p and tolerance zone using EQ.4.

4.2 Simplex-Containment Fit

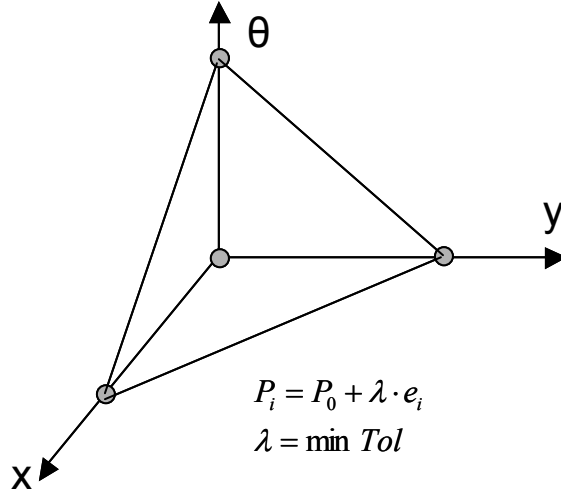


Figure 6 Initial positions for a simplex method

To minimize the objective function as defined in EQ.3, there are multiple methods that can be employed. In this paper, we choose the simplex method [21] because it is simple to implement and the end result is also less sensitive to initial condition since it samples $N+1$ points in the transformation space where N is the dimension of the transformation space.

The simplex method starts with a set of initial vertices. It computes the objective function for all the vertices. It then compares the objective values and determines whether to expand or contract the simplex by moving the vertex with the highest objective function value. The initial position of the simplex vertices can be set by the following equation.

$$P_i = P_0 + \lambda \cdot e_i$$

where P_0 is at the original point in the transformation space, e_i is the principal axis vector. The initial step length λ is set to be the minimal tolerance.

The least-squares based best fit provides a transformation to align inspection data closely with nominal model, even though such as transformation itself may not directly lead to the inspection data falling within tolerance zone. However, such a transformation can reduce the number of iterations the simplex method needs to converge. One of the most computationally intensive procedures in the simplex method is the closest-distance calculation between inspection data and nominal shape. The least-squares based method provides an initial position for alignment, which would lead to a significant amount of time saving in simplex search. Our experimental result will further demonstrate that.

Another input for the simplex method that can be helpful for the computing time saving is the initial vertices in the simplex. After we have calculated the shape of the admissible transformation volume for the nominal geometry, we can sample this ATV into several

points, which would then be the initial vertices for the manufactured part's ATV computing. This is based on the proposition in the last section, that a nominal shape's ATV provides bounds for actual shape's ATV.

4.3 Marching Cubes and ATV Computing

The containment function gives a precise mathematical description of the iso-surfaces of target containment objective function values in the transformation surface. To help visualize the containment function and quantify the ATV size, we use the Marching Cubes algorithm [17]. The marching cubes algorithm is an efficient algorithm to rapidly approximate a mathematical surface with a set of polygons in a given function governing space. The result of the marching cubes algorithm is a surface that approximates the iso-surface that is constant throughout the field.

In order to obtain a polygon representation for an iso-surface using the Marching Cubes algorithm, we need to determine the location, size bound and resolution of the cubes of the iso-surface in the transformation space.

The original point in the transformation space can be used as the center point in locating the nominal geometry's ATV. After a least-squares based best-fit aligns the manufactured part close to the nominal shape, the original point can also be a good location for the manufactured part's ATV computing. For the nominal shape's ATV, the sizes of the tolerances provide a good bound for polygonal representation of ATV. For the manufactured shape's ATV, we can use the same tolerance or the nominal shape's ATV's as the bounds. The smoothness of the ATV depends on the cube resolution.

To have a characterization of the size of the ATV, we compute the extremes values along the principal axes. We iterate through all the cubes. For each potential triangle within each cube, we compute the extreme values. Based on these extreme values, we then form a boundary box for the ATV.

5 Implementation and Examples

A system for part conformance check based on the ATV concept has been developed on an HP-UX 11.0 machine. It has the following components:

- Fletcher-Powell minimization module, minimizing the objective functions according to the calculated gradient [13]. We use this method to find a least-squares optimal transformation to minimize RMS (root-mean-square) error between nominal shape and manufactured shape.
- Simplex optimization module, minimizing the objective functions by moving the simplex vertices in an N-dimensional space. We use this method for a final containment fit.

- Tolerance zone representation module, representing tolerance zone as a function of nominal geometry. We use this representation to facilitate the computing of containment fit objective function under a given transformation of inspection data.
- Marching Cubes module, computing the approximate polygons for iso-surfaces and visualizing the iso-surface and the ATV in transformation space.

In this paper, to demonstrate the flexibility of applying our ATV in different tolerance applications, we present three examples with dimensional tolerance, positional tolerance and non-uniform profile tolerance specifications respectively. Through these examples, we highlight 1) how containment fitting is used for part tolerance conformance check, 2) how the ATV is used for quantitative evaluation of manufactured part dimensional quality, and how well the manufactured part fits into the design specified tolerance zone. We will also compare our method with other methods in inspection data analysis.

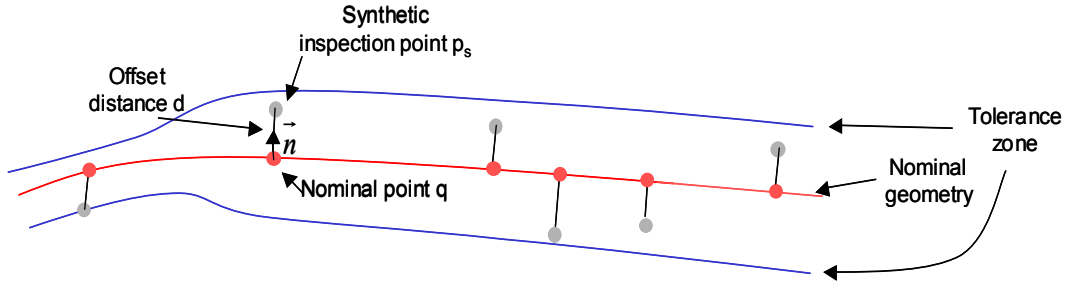


Figure 7 Synthetic inspection point creation

In order to have a ground truth for evaluating these methods, we used the synthetic inspection points. These synthetic points were created from the offsetting of nominal points by a random distance d (Figure 7). For each nominal point q , we find its normal direction \vec{n} on the nominal surface and its tolerance δ . So a synthetic point, p_s , from a nominal point q , can be obtained from a deviation coefficient c and a random function r . Mathematically, it can be represented as

$$p_s = q + c * \vec{n} * \delta * r \quad \text{EQ. 6}$$

Here C is an adjusted deviation coefficient based on the maximum sample r value so that the maximum deviation from the nominal model is either $q + c * \vec{n} * \delta$ or $q - c * \vec{n} * \delta$. When deviation coefficient $C=0$, the synthetic points lie exactly on the nominal shape. As deviation coefficient C increases, the synthetic points deviates more from the nominal shape. When deviation coefficient $C=0.5$, the synthetic points are just within the tolerance zone. When the deviation coefficient $C>0.5$, some of the synthetic points are outside of the tolerance boundaries.

In the rest of this section, we describe the following:

- examples of different tolerance specifications used in this study,

- results of simplex-containment fit on these examples,
- comparison of iso-surface and the calculated ATV,
- further discussion on the choice of containment fit objective functions and the initial position for ATV calculation.

5.1 Description of three examples of different tolerances

We first describe the three tolerance examples. We then describe how containment fit and ATV were used to in part quality inspection analysis. All the tolerance examples presented in this paper has two or three degrees of freedom. However, the methodology developed in this paper is applicable to 3D examples of more degrees of freedom.

5.1.1 Example 1 Dimensional tolerance for a hole diameter

A 2D hole with diameter 4.0 and dimensional tolerance $[-0.4, 0.4]$ is shown in Figure 8.a. Shown in Figure 8.b is a synthetic inspection data fitting into the tolerance zone. In this example, there are 100 synthetic inspection points.

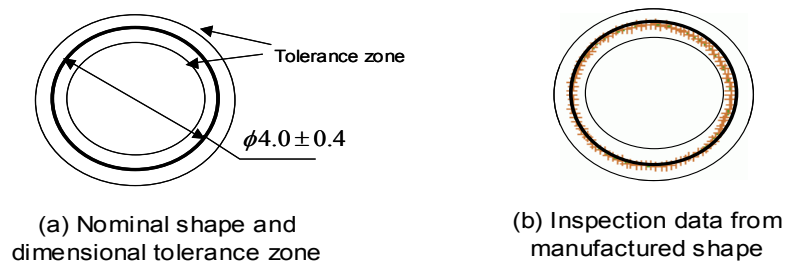


Figure 8 Hole dimensional tolerance

5.1.2 Example 2 Positional tolerances on 4 holes

Figure 9 shows a four-hole positional tolerance at maximum material condition, a classical example in simultaneous tolerance control. The four holes have diameter 4.0. The manufactured four holes should simultaneously fit into a tolerance zone. In this example, there are 400 synthetic inspection points.

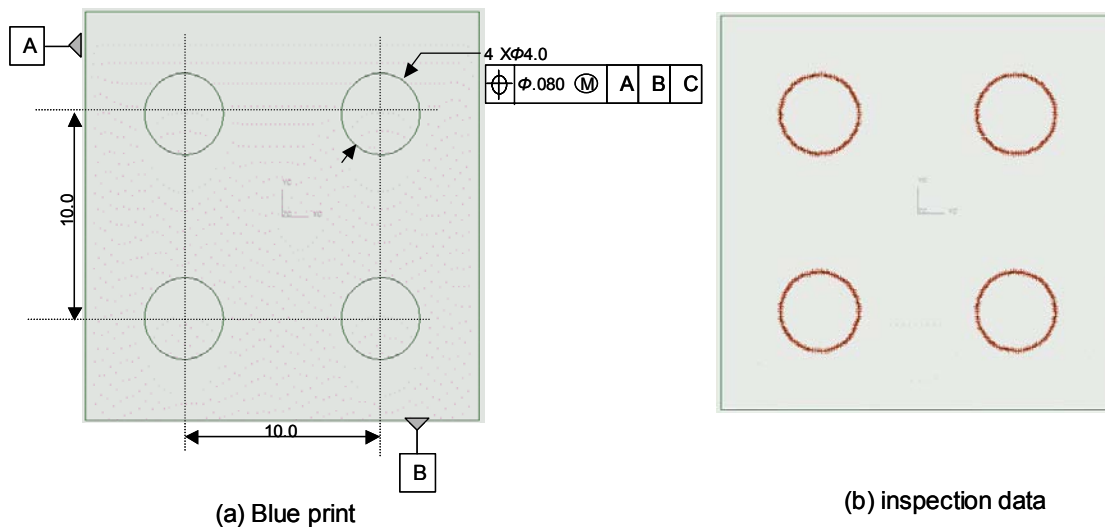


Figure 9 Positional tolerance for four holes

5.1.3 Example 3 Non-uniform profile tolerances

Figure 10 shows a dovetail part used in an aircraft engine. To ensure the even load among the pressure surfaces for the dovetail, there is a tighter profile tolerance on the pressure surface (0.001 mil). For the non-critical surfaces, the profile tolerances are relatively looser. It should be noted that the specific tolerance values in Figure 10 have been altered from the true values used in dovetail manufacturing. In this example, there are 300 synthetic inspection points. The original geometric entities in the surface profile are either an arc or a straight line. We constructed a NURBS curve through these lines and arcs. We then associated each tolerance with a parametric segment in the NURBS curve. Thus, we have a parametric representation of tolerance zone.

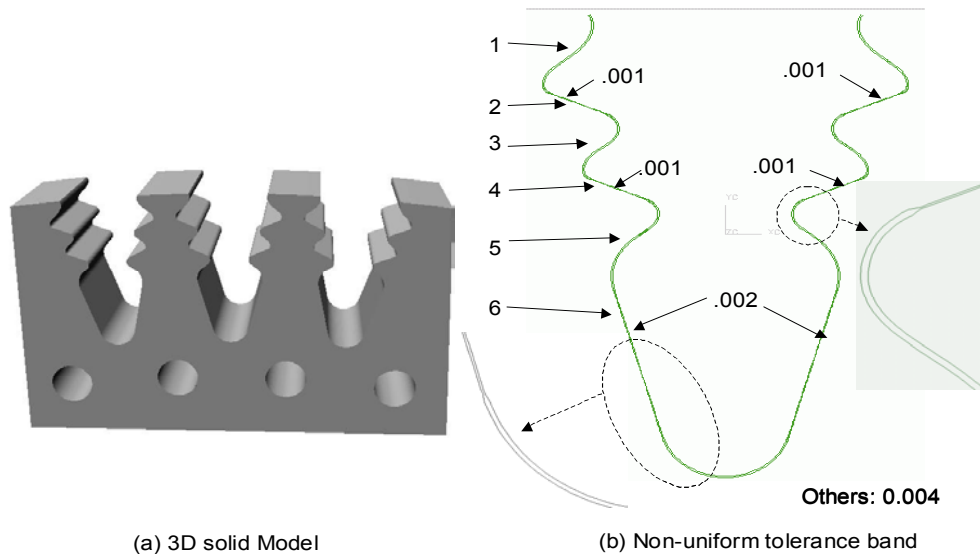


Figure 10 Non-uniform profile tolerances

5.2 Simplex-Containment fit

5.2.1 Results of simplex-containment fit

Non-uniform profile tolerance

We selected the non-uniform profile tolerance (Figure 10) as an example for comparing containment fit, least-squares fit and mini-max fit since it is the most complex one out of the three tolerance examples. In this example, the $\lambda=0.001$ was chosen for our simplex method. We tested these methods under different initial positions to examine the robustness of various methods. The points at different initial positions were created by the transformation of synthetic points. The synthetic points were created in the nominal geometry's coordinate system (EQ.7). The transformation (x, y, θ) is a point in the transformation space, representing the amount of translation in x-axis and y-axis and the rotation θ around z-axis applied upon the synthetic points.

Three methods, total least-squares fit, mini-max fit, and containment fit were used to check if a given inspection data meets the specified tolerances. The specific test examples include $c=0.40$, 0.48 , 0.499 , and 0.51 . We also created synthetic points from nominal geometry of selected particular tolerance bands (Figure 10).

Table 1 Testing results at initial condition (0, 0, 0)

Test Cases	Expected result	LS fit	Mini-max fit	Simplex-Containment fit
0.4 random	Y	Y	Y	Y
0.48 random	Y	N	Y	Y
0.499 random	Y	N	N	Y
0.51 random	N	N	N	N
0.48 - 1	Y	N	Y	Y
0.48 -6	Y	Y	N	Y
0.48 -1- 6	Y	N	N	Y

Table 2 Testing results at initial condition (0.001, -0.001, 1)

Test Cases	Expected result	LS fit	Mini-max fit	Simplex-Containment fit
0.4 random	Y	Y	Y	Y
0.48 random	Y	N	Y	Y
0.499 random	Y	N	N	Y
0.51 random	N	N	N	N
0.48 - 1	Y	N	Y	Y
0.48 -6	Y	Y	N	Y
0.48 -1- 6	Y	N	N	Y

Table 3 Testing results at initial condition (0.005, -0.005, 5)

Test Cases	Expected result	LS fit	Mini-max fit	Simplex-Containment fit
------------	-----------------	--------	--------------	-------------------------

0.4 random	Y	Y	Y	Y
0.48 random	Y	N	Y	Y
0.499 random	Y	N	N	Y
0.51 random	N	N	N	N
0.48 - 1	Y	N	Y	Y
0.48 -6	Y	Y	N	Y
0.48 -1- 6	Y	N	N	Y

We listed the results from the three methods under different initial conditions in Table 1, Table 2, and Table 3. The (x, y, θ) for three initial conditions are $(0, 0, 0)$, $(0.001, -0.001, 1 \cdot \pi/180)$ and $(0.005, -0.05, 5 \cdot \pi/180)$. In all the three tables, Column 1 refers to the deviation coefficient C . For example, “0.4 random” refers to points are randomly created for all the tolerance bands. “0.48 -1-6” refers to points are randomly created only for tolerance band 1 and band 6 and points in the other tolerance bands remain nominal. Column 2 lists the expected part conformance results. That is, when the deviation coefficient C is smaller than 0.5, the part is expected to pass the tolerance test. When C is larger than 0.5, it is expected to fail in the tolerance test. Column 3, Column 4 and Column 5 list the results obtained from three best-fit methods: least-squares, mini-max, and containment fit.

As the results in the three tables (Table1, Table2, Table3) show, *under various initial conditions, only containment fit using a simplex optimization method gives results consistent with the expected results*. Both total least-squares and mini-max fitting give false pass/fail part conformance checks in some cases. The least-squares method led to false results when the c is 0.48 and 0.49 for all tolerance bands, and for the case when there are deviations only at band 1 and band 6. Likewise, the mini-max fit method created false results when the c is 0.499 under all three initial conditions, and the cases when there are deviations only at band 1 and band 6, or only at band 6.

Table 4 Containment function evaluation times

Test Cases	W/O LF FIT	W LS FIT
0.4 random	109	22
0.48 random	134	34
0.499 random	158	64
0.51 random	251	148
0.48 - 1	114	33
0.48 -6	100	16
0.48 -1- 6	153	49

In the iterative simplex search process, the time of calculating the objective function from an inspection point to nominal geometry is large. So we compare the objective function invoking times during the simplex converging process. The number of containment function calculation times in the simplex method with and without the initial least-squares fit is shown in Table 4 for the initial condition (0.005, -0.05, 5). With or without the initial least squares best fit, simplex method gave the correct results. As revealed in this table, *when the initial position is far off from the nominal shape, a least squares fit in combination with a simplex fit would reduce the number of times it needs for the simplex method to converge.*

Position Tolerance

To further evaluate the iterative times in simplex search for different manufactured shapes, we examined the method for the four-hole position tolerance at maximum material condition (Figure 9).

Table 5 shows how the simplex method converges for different manufactured shapes (i.e. with different deviations from nominal shape) and at different initial position for the positional tolerance example. During the simplex search process, we set the step length to be 0.01 and terminating tolerance (the difference of objective function values at simplex vertices) $ftol=1.0e-8$. Table 5 lists the times of containment function calculation it takes for a simplex method to converge. The numbers with asterisk (*) sign mean that a simplex re-initialization process was invoked. The times are the combined containment function invoking times. The initiation condition listed in the Column 1 in the table is a point in the transformation space. That is, a transformation is applied to the synthetic points so they are away from the tolerance zone. The results in this table show, *as the manufactured part moves further away from tolerance zone, more time it takes for the method to converge. When the part is out of tolerance specification, it takes significantly more times to converge.*

Table 5 Containment function evaluation times in simplex-containment fit

Initial condition	Nom	C=0.40	C=0.48	C=0.499	C=0.60
(0,0,0)	2	10	24	31	589*
(0.001, -0.001, 1)	12	40	65	66	702*
(0.002, -0.002, 2)	18	36	50	51	417*
(0.003, -0.003, 3)	21	44	46	50	477*
(0.004, -0.004, 4)	27	64	78	76	572*
(0.005, -0.005, 5)	31	86	96	90	654*
(0.005, -0.05, 5)	27	87	94	87	501*
(0.005, 0.005, 5)	58	383*	560*	348	718*

5.3 ATV calculation in transformation space

5.3.1 ATV computing

To further quantify the part dimensional quality and examine how well the manufactured part fits within the design tolerance zone, we present the results of using iso-surfaces and ATVs for dimensional quality analysis.

Figure 11 shows the rendered image and wire-frame image of the nominal shape's ATV for the hole's diameter tolerance. Figure 12 shows the iso-surfaces for a variety of holes with different deviations from the nominal shape. C is the deviation coefficient, changing from 0 to 0.60. The containment function values of the iso-surfaces are 0.075131, 0.56447, 0.000937 and 0.000000. The last iso-surfaces and the enclosed area at column $f=0.000000$ corresponds to the ATV shapes. We used $20*20*20$ voxels in the (x, y, θ) transformation space (with x ranging in $[-0.05, 0.05]$, y ranging in $[-0.05, 0.05]$ and θ ranging in $[-0.007, 0.007]$) to visualize the iso-surface and the ATV. As it is shown in Figure 12, the nominal shape has a much larger ATV than the manufactured shape does. Since the shape is a 2D hole, there are only two effective degrees of freedom. Due to the synthesized shape is close to a circle, so the rotation around the hole center does not change the iso-surface.

Figure 13 shows the rendered image and wire-frame image of the nominal shape's ATV for the four-hole position tolerance. Figure 14 shows a set of iso-surfaces for shapes with different deviation coefficients $C=0.00, 0.40, 0.48, 0.499, \text{ and } 0.60$. The respective objective functions are 0.177156, 0.121000, 0.007628, and 0.000000. The last iso-surfaces and the enclosed area at column $f=0.000000$ corresponds to the ATV shapes. We also used $20*20*20$ voxels in the transformation space with x ranging in $[-0.05, 0.05]$, y ranging in $[-0.05, 0.05]$ and θ ranging in $[-0.007, 0.007]$ to visualize the iso-surface and the ATV.

Figure 15 shows the rendered image and wire-frame image of the nominal shape's ATV for the four-hole position tolerance. Figure 16 shows a set of iso-surfaces for shapes with different deviation coefficients $C=0.00, 0.40, 0.48, 0.499, \text{ and } 0.60$. The respective objective functions are 0.000328, 0.000049, 0.000010, and 0.000000. The last iso-surfaces and the enclosed area at column $f=0.000000$ corresponds to the ATV shapes. We used $16*16*16$ voxel in the transformation space with x ranging in $[-0.0016, 0.00016]$, y ranging in $[-0.0016, 0.0016]$, and θ ranging in $[-0.0032, 0.0032]$ to visualize the iso-surface and the ATV. As it is shown in the figure, the nominal shape's iso-surface is larger than any other surfaces at the same iso-surface value. Likewise, the admissible iso-surface (in the last column) for the nominal shape is also larger than all other shapes. The admissible iso-surface when c is 0.51 is null, which indicated that the admissible volume is null and the part is not conformal to tolerance specifications.

Beside the iso-surface calculation for the containment function and the ATV modeling, we also quantitatively compared the boundary boxes of the ATVs (minimum and maximum values along the three axes). They are listed in Table 6, Table 7, and Table 8. These three tables are respectively corresponding to the tolerances in the three examples. As revealed in these three tables, as the deviation coefficient increases, the minimal values of the ATV become smaller and the maximum values of the ATV become larger. The distance between the minimal and maximum values along each axis is getting smaller as the deviation coefficient C increases. Thus, we can use ATV to characterize how far manufactured shape deviates from nominal shape w.r.t the tolerance zone. That is to say, *when a manufactured shape deviates more from the nominal shape, the ATV becomes smaller*. Note, in some adjacent rows (for example, when $C=0.48$ and $C=0.499$ in Table 6), the mini-max values are the same. This is due to the transformation space sampling resolution.

Table 6 Mini-max values of ATV for a dimensional tolerance

C	X		Y		Z	
	min	max	min	Max	Min	max
0.00	-0.037500	0.043750	-0.037500	0.043750	-0.007000	0.007000
0.40	-0.006250	0.006250	-0.006250	0.006250	-0.007000	0.007000
0.48	-0.000000	0.000000	-0.000000	0.000000	-0.007000	0.007000
0.499	-0.000000	0.000000	-0.000000	0.000000	-0.007000	0.007000

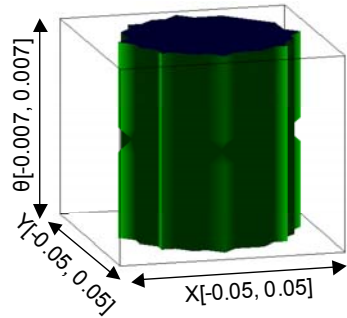
Table 7 Mini-max values of ATV for a positional tolerance

C	X		Y		Z	
	min	max	min	max	Min	max
0.00	-0.031250	0.037500	-0.031250	0.037500	-0.005250	0.006125
0.40	-0.006250	0.006250	-0.000000	0.006250	-0.000875	0.001750
0.48	-0.000000	0.000000	-0.000000	0.000000	-0.000000	0.000000
0.499	-0.000000	0.000000	-0.000000	0.000000	-0.000000	0.000000

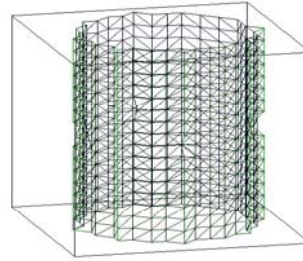
Table 8 Mini-max values of ATV for a profile tolerance

C	X		Y		Z	
	min	max	min	max	Min	max
0.00	-0.001000	0.001000	-0.000600	0.000602	-0.001201	0.001201

0.40	-0.000200	0.000200	-0.000000	0.000046	-0.000401	0.000001
0.48	-0.000000	0.000000	-0.000000	0.000010	-0.000001	0.000001
0.499	-0.000000	0.000000	-0.000000	0.000000	-0.000000	0.000001



(a) ATV for nominal shape



(b) ATV for manufactured shape

Figure 11 ATV for the dimensional tolerance

f	0.075131	0.056447	0.000937	0.000000
C0.00				
C0.40				
C0.48				Small point
C0.499				Small point
C0.60			null	null

Figure 12 Iso-surfaces in transformation space for a dimensional tolerance

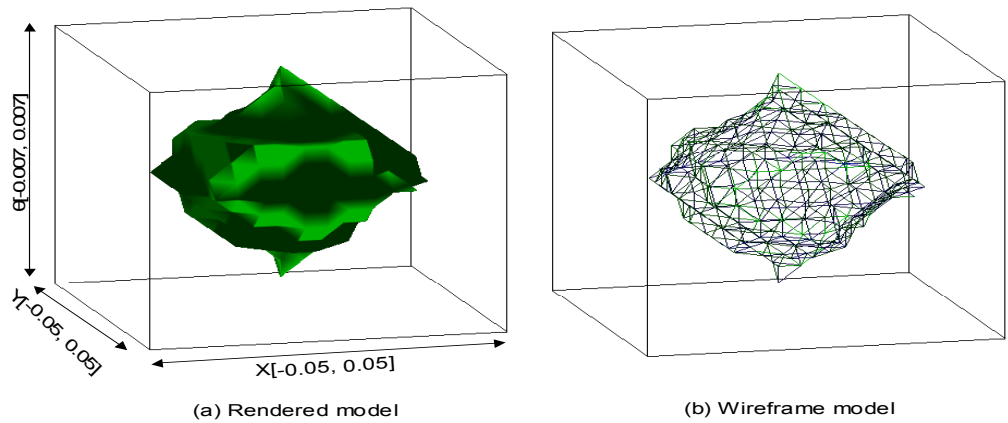


Figure 13 ATV for the positional tolerance

f	0.177156	0.121000	0.007628	0.000000
C0.00				
C0.40				
C0.48				Small point
C0.499				Small point
C0.60			null	null

Figure 14 Iso- surfaces in transformation space for positional tolerances

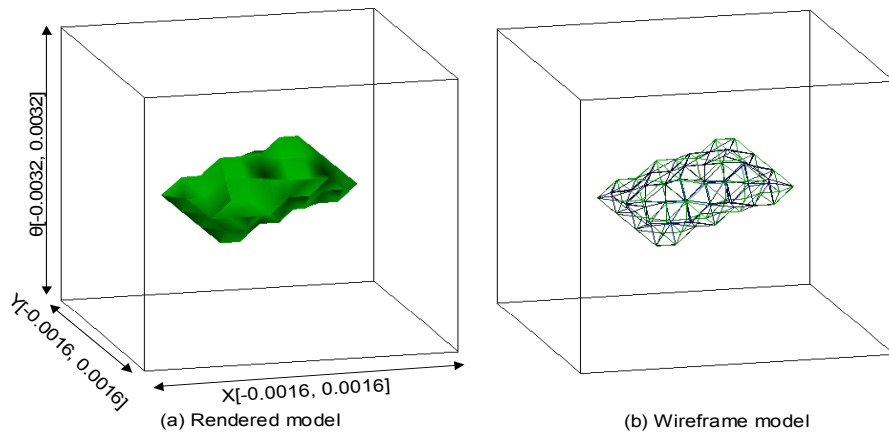


Figure 15 ATV for the profile tolerance

f	0.000328	0.000049	0.000010	0.00000
Nominal				
0.40				
0.48				A small point
0.499				A small point
0.51			null	null

Figure 16 Iso-surfaces in transformation space for profile tolerances

5.4 Further discussions on containment fit and ATV calculation

We have examined how to use containment fit and ATV for inspection data analysis. We then further experimentally evaluated 1) the impact of different objective functions on the containment fit and iso-surfaces in the transformation space, and 2) the effect of the initial position of an inspection data set on the ATV.

Different objective functions (different m) lead to the same result, even though the iso-surface is different when the objective function is larger than zero. However, the shape of the ATVs remains the same.

Table 9 compares the containment function invoking times for different objective functions, respectively $m=1, 2$ and 3 for EQ.3 for the four-hole position tolerance example. We compared the computing times for two sets of shapes with deviation coefficients $C=0.48$ and $C=0.499$. There are no major differences in terms of the computing times. Even though, with the increased order of m , the gradient function becomes steeper which would be less likely for the simplex search to get stuck in a local neighborhood. For example, when $C=0.48, m=2$ at initial condition $(0.005, 0.005, 5)$, the re-initialization process was invoked. After the re-initialization, it took 27 times for the simplex iteration process to terminate.

Table 9 Different objective functions for simplex-containment fit

Initial condition	C0.48- m=1	C0.48- m=2	C0.48- m=3	C0.499- m=1	C0.499- m=2	C0.499- m=3
0	31	24	24	33	31	33
(0.001, - 0.001, 1)	66	65	64	164	66	66
(0.002, - 0.002, 2)	51	50	50	101	51	51
(0.003, - 0.003, 3)	50	46	60	73	50	59
(0.004, - 0.004, 4)	76	78	60	74	76	74
(0.005, - 0.005, 5)	90	96	70	70	90	77
(0.005, - 0.05, 5)	87	94	92	70	87	90
(0.005, 0.005, 5)	348	560-27	109	71	348	124

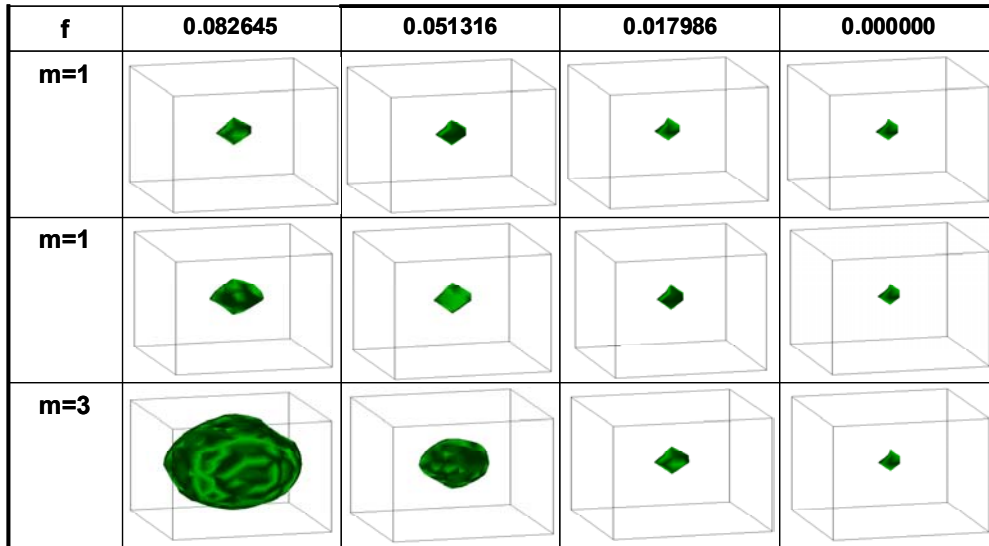


Figure 17 Iso-surfaces for different objective functions

Figure 17 shows the iso-surfaces when $C=0.40$ for a set of different objective functions. As predicted, higher m leads to a larger gradient. It is exhibited in the figure as the large deviations of the iso-surface shapes between two adjacent objective function values. Corresponding to EQ.3, $m=1, 2, 3$ are listed in the 1st column. The objective function values are 0.082645, 0.051316, 0.017986 and 0.000000. As expected, the ATVs are the same for different objective functions. In all three cases when $m=1, 2, 3$, the boundary boxes of the ATVs are the same, with x ranging in $[-0.000200, 0.000200]$, y ranging in $[-0.000200, 0.000200]$, θ ranging in $[-0.000400, 0.000800]$. The experiment indicates that the higher m is, the larger gradient is and the less likely we need to re-initialize the simplex during the iteration process.

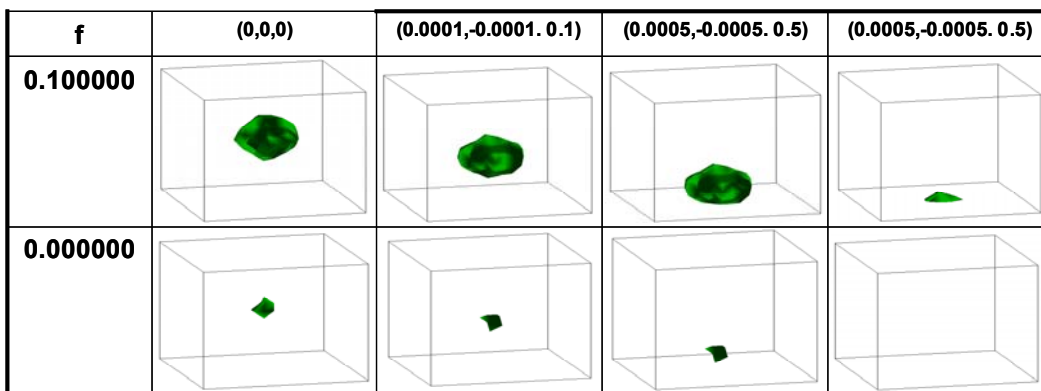


Figure 18 Iso-surfaces at different initial conditions

Figure 18 Shows a set of iso-surface and ATV for the four holes when $C=0.40$ at a variety of initial positions. These initial positions are the positions of the four holes from the initial position with a translation and rotation at $(0, 0, 0)$, $(0.0001, -0.0001, 0.1)$, $(0.0005, -0.0005, 0.5)$ and $(0.0005, -0.0005, 0.5)$. As shown in this figure, *inspection data at different initial positions do not change the shape of the iso-surface or ATV, even though the ATV position and orientation may change.* In this particular case, the iso-surface is moving along the negative axis of angle theta in the transformation space.

6 Conclusions

This paper presents a new approach for inspection data analysis based on a novel concept, *admissible transformation volume*. Two basic analysis issues in coordinate metrology, qualitative part conformance check and quantitative quality evaluation, are studied from the perspective of admissible transformation. Theories and algorithms on how to compute and apply the ATV for inspection data analysis are presented.

Three examples involving hole diameter, positional tolerance, and non-uniform profile tolerances are presented. Experimental results on these examples demonstrate that ATV provides an effective means for inspection data analysis. It is especially useful for the inspection of shapes with complex tolerance zones where many traditional data analysis methods often do not produce correct results. An ATV is an intrinsic property between design tolerance specifications and the manufactured part shape. It is invariant to the objective function or coordinate system for the measurement data. In addition, the size of ATV in the transformation space is indicative of the amount of deviation between the nominal shape and the manufactured part shape. It is particularly effective for complex shape gauging when conventional minimum tolerance zone calculation is not applicable.

A potential challenge to ATV computing is with “floating” tolerance zones such as a cylindricity tolerance, in which the specific tolerance zone is not defined even though the radii difference is defined. Our future work is to adopt a scalable representation of tolerance zones to address this kind of issues.

References:

1. American National Standard ASME Y14.5M, *Dimensioning and Tolerancing*, The American Society of Mechanical Engineers, New York, 1994.
2. Barequet, G., Briggs, A.J., Dickerson, M.T., and Goodrich, M.T., “Offset-polygon annulus placement problems,” *Computational Geometry: Theory and Applications* (CGTA), vol. 11 No. 3-4, pp. 125-141, 1998.
3. Boothby, W. M., *An introduction to differentiable manifolds and Riemannian geometry*, Academic Press, Orlando, Fla, 2d edition, 1986.

4. Carpinetti, L. C. R. and Chetwynd, D. G., "Genetic search methods for assessing geometric tolerances," *Computer Methods in Applied Mechanics and Engineering*, Vol. 122, pp. 193-204, 1995.
5. Chirikjian, G. S. and Zhou, S., "Metrics on Motion and Deformation of Solid Models," ASME Transactions *Journal of Mechanical Design*, Vol. 120, pp 252-261, 1998.
6. Choi, W. and Kurfess, T. R., "Dimensional Measurement Data Analysis, Part 1: A Zone Fitting Algorithm," ASME Transactions *Journal of Manufacturing Science and Engineering*, Vol. 121, pp. 238 – 245, 1999.
7. Choi, W. and Kurfess, T. R., "Dimensional Measurement Data Analysis, Part 2: Minimum Zone Evaluation," ASME Transactions *Journal of Manufacturing Science and Engineering*, Vol. 121, pp. 246 – 250, 1999.
8. Clement, A., Valade, C., Riviere, A., "The TTRSs: 13 Oriented Constraints for Dimensioning, Tolerancing and Inspection," *Advanced Mathematical Tools in Metrology III*, Berlin, pp. 24–41, September 25–28, 1996.
9. Damodarasamy, S., and Anand, S., "Evaluation of Minimum Zone for Flatness by Normal Plane Method and Simplex Search," *IIE Transactions*, Vol. 31, pp. 617–626, 1999.
10. Davidson, J. K., Mujezinovic, A., and Shah, J. J., "A New Mathematical Model for Geometric Tolerances as Applied to Round Faces," ASME Transactions *Journal of Mechanical Design*, Vol. 124, pp. 609 – 622, 2002.
11. Endrias, D. H and Feng, H. Y., "Minimum-Zone Form Tolerance Evaluation Using Rigid-Body Coordinate Transformation," ASME Transactions *Journal of Computing and Information Science in Engineering*, Vol. 3, pp. 31 – 38, 2003
12. Feng, S. C. and Hopp, T. H., "A Review of Current Geometric Tolerancing Theories and Inspection Data Analysis Algorithms," NISTIR 4509, 1991.
13. Fletcher, R. and Powell, M. J. D., "A rapidly convergent descent method for minimization", *Computer Journal*, Vol. 6, pp. 163 – 168, 1963.
14. Huang, S. T., Fan, K. C., and Wu, J. H., "A New Minimum Zone Method for Evaluating Straightness Errors," *Precision Engineering*, Vol. 15, pp. 158 – 165, 1993.
15. Kaiser, M. J., Cheraghi, S. H. and Li, S., "The structure of positional tolerance evaluation: I Constructive geometric approach," *Computer Methods in Applied Mechanics and Engineering*, Vol. 190, pp. 149-178, 2000.

16. Lai, H. Y., Jywe, W. Y., Chen, C. K., and Liu, C. H., "Precision Modeling of Form Errors for Cylindricity Evaluation Using Genetic Algorithms," *Precision Engineering*, Vol. 24, pp. 310–319, 2000.
17. Lorensen, W. E. and Cline, H. E., "Marching Cubes: A High Resolution 3D Surface Construction Algorithm," *Computer Graphics* (Proceedings of SIGGRAPH '87), Vol. 21, No. 4, pp. 163-169, 1987.
18. Menq, C. H., Yao, H. T., and Lai, G. Y., "Automated Precision Measurement of Surface Profile in CAD-Directed Inspection," *IEEE Transactions on Robotics and Automation*, Vol. 8, No. 2, pp. 268-278, 1992.
19. Murthy, T. S. R., and Abdin, S. Z., "Minimum Zone Evaluation of Surfaces," *International Journal of Machine Tools and Manufacture*, Vol. 20, pp. 123–136, 1980.
20. Pasupathy, T. M. K., Morse, E. P., and Wilhelm, R. G., "A Survey of Mathematical Methods for the Construction of Geometric Tolerance Zones," *ASME Transactions Journal of Computing and Information Science in Engineering*, Vol. 3, pp. 64 – 75, 2003.
21. Press, W. H., Teukolsky, S. A., Vetterling, W. T., and Flannery, B. P., *Numerical Recipes in C: The Art of Scientific Computing*, 2nd ed., Cambridge University Press, New York, 1992.
22. Ranade, S., Lehtihet, E.A., and Cavalier, T.M, "On the Producibility of Composite Tolerance Specifications for Patterns of Holes," *International Journal of Production Research*, Vol. 39, No. 7, pp.1305-1321, 2001.
23. Requicha, A. A. G., "Towards a Theory of Geometric Tolerances," *Internal Journal of Robotics Research*, Vol. 2, No. 4, pp. 45-60, 1983.
24. Roy, U. and Li, B., 1998, "Representation and Interpretation of Geometric Tolerances for Polyhedral Objects—I. Form Tolerances," *Computer-Aided Design*, Vol. 30, No.2, pp. 151–161, 1998.
25. Roy, U. and Zhang, X., "Establishment of a Pair of Concentric Circles with the Minimum Radial Separation for Assessing Roundness Error," *Computer-Aided Design*, Vol. 24, No. 3, pp. 161–168, 1992.
26. Shah, J. J. and Zhang, B., "Attribute Graph Model for Geometric Tolerancing," *Proceedings of 18th ASME Design Automation Conferences*, Scottsdale, AZ, Sep 13- 16, Vol. H0770B, pp. 133 – 139, 1992.
27. Turner, J. U. and Wozny, M. J., "The M-space Theory of Tolerances," *Proceedings of the ASME 16th Design Automation Conference*, Chicago, IL, pp. 217–225, 1990.

28. Xi, M., Lehtihet, E.A., and Cavalier, T.M., "A Mathematical Optimization Approach to a Subset of Tolerance Transfer Problems," ASME Transactions *Journal of Computing and Information Science in Engineering* Vol. 1, No. 2, pp. 180-185, 2001.
29. Wu Y., Shah J., and Davidson J., "Computer Modeling of Geometric Variations in Mechanical Parts and Assemblies," ASME Transactions *Journal of Computing and Information Science in Engineering*, Vol. 3 No. 2, 2003.